Chapter III.14

CERN beamline for fixed-target experiments

Alexander Gerbershagen
PARTREC, University Medical Center Groningen, University of Groningen, Groningen, Netherlands

Fixed-target experiments are continuing to play a major role in the very beginnings of accelerator-based studies in particle physics. While collider experiments dominate the exploration in the high-energy domain, fixed-target experiments still cover the important complementary domain, as they permit experiments with extremely high event rates. In addition, they play a crucial role in detector prototype testing and calibration, as well as radiation-hardness tests. This chapter summarises the purpose of the fixed-target beam lines, focusing on the beam lines present at CERN. It explains the basics of beam interaction with the target and the production of secondary particles, illustrates the design of secondary and tertiary beam lines and presents examples of experiments at CERN East and North Experimental Areas.

Modern high-energy physics began with the fixed-target experiments—starting from Rutherford's gold foil experiment, over the first accelerator-based experiments and the discovery of J/Ψ particle [1,2]. However, in the 1970's experiments at colliders such as the Intersecting Storage Rings (ISR) at CERN [3] and the Tevatron at Fermilab [4] became possible, mostly due to the technological improvements enabling better beam focusing and steering. The centre-of-mass energy of the collisions of two beams with equal particle masses and energies increases linearly with the energy of the individual beams. In fixed-target experiments the centre-of-mass energy increases only with the square root of the beam energy, hence making exploration of high-energy domain more challenging. However, fixed-target experiments remain attractive, as they offer higher event rates, easier installation and access, pose less space restrictions and can offer a large momentum range and beams that are flexible in regard to the particle types. Realising the potential benefits for the physics experiments aimed at the observation of extremely seldom processes, for detector prototype testing and calibration as well as for material irradiations, CERN management has launched in 2018 the Physics Beyond Colliders programme (logo displayed in Fig. III.14.1) [5–7] to explore the possibilities of CERN accelerator complex that are complementary to the construction of new large high-energy colliders. A big share of this program concerns work in the CERN North Area, that operates with beams from the Super Proton Synchrotron (SPS) of 400 GeV momentum and five-second long slow extraction spills, and encompasses a large share of CERN's fixed-target beam lines with a total beam line length of about seven kilometres.

This chapter should be cited as: CERN beamline for fixed target experiments, A. Gerbershagen, DOI: 10.23730/CYRSP-2024-003.2155, in: Proceedings of the Joint Universities Accelerator School (JUAS): Courses and exercises, E. Métral (ed.), CERN Yellow Reports: School Proceedings, CERN-2024-003, DOI: 10.23730/CYRSP-2024-003, p. 2155.

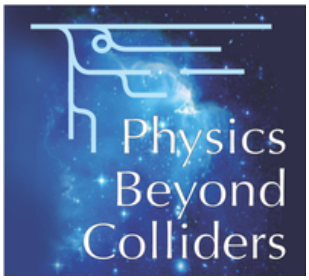

Fig. III.14.1: Logo of Physics Beyond Colliders programme [8].

III.14.1 Examples of fixed-target setups at CERN

There is a wide portfolio of fixed-target setups at CERN, which largely fall into three categories:

- Large fixed-target experiments, that include examples like
  - COMPASS [9] and AMBER [10] that examine quantum chromodynamics (QCD) properties of hadrons and measure QCD constants,
  - NA61 [11] experiment with heavy-ion beams that measures hadronic final states,
  - NA62 [12] that measures the ultra-rare kaon decay in search of physics beyond Standard Model,
  - NA64 [12] searching for dark matter,
  - CLOUD [14] that examines the influence of irradiation on the formation of the clouds.
- Irradiation facilities
  - CHARM and IRRAD in the East Area,
  - GIF++ and HiRadMat in the North Area.
- And finally the beam lines for test beams
  - T9 and T10 in the East Area,
  - H2, H4, H6 and H8 in the North Area.

In addition, a large number of facilities for specific research purposes are operating with secondary beams, such as the Neutron Time-Of-Flight (n_TOF) for neutron beam research, the Advanced WAKE-field Experiment (AWAKE) studying new accelerator methods with help of plasma wakefields, the Antiproton Decelerator (AD) and the Extra Low ENergy Antiproton ring (ELENA) for antimatter research, ISOLDE for heavy-ion research, etc.

III.14.2 Secondary particle production

The principle of secondary particle production is taken from the processes naturally occurring in the upper layers of the atmosphere (illustrated in Fig III.14.2). The high-energy protons interact with the nuclei of matter, mostly via the strong interaction, as it is the dominant cross-section at the energies of tens or hundreds of GeV. This triggers a hadronic cascade, in which hadrons (pions, kaons, neutrons, protons, antiprotons and heavier particles) are produced from the kinetic energy of the initial beam. Some

of those particles, like protons or neutrons, are long-lived, while others, like neutral pions, decay almost instantaneously. The latter decay into two high-energy photons, which, in turn, produce electron-positron pairs when propagating in matter. The electrons and positrons can further emit Bremsstrahlung, that can trigger further electron-positron pair production. That constitutes the electromagnetic cascade.

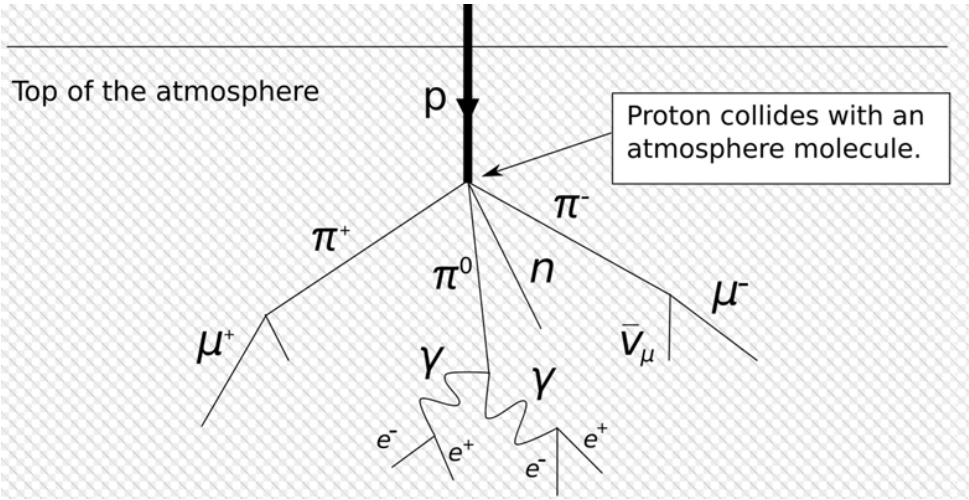

Fig. III.14.2: Illustration of secondary particle production principle [15].

As Fig. III.14.2 illustrates, after the interaction with the target the beam that was initially composed only of protons, contains all possible hadrons and leptons that have been produced at the target and in the subsequent decay of the particles. That beam is referred to as a secondary beam, while the initisal proton beam is called primary beam.

CERN East [16,17] and North [18] Experimental Areas utilize beryllium targets of various lengths for the production of secondary particles. beryllium has been chosen as material because of its comparably high radiation length $X_0 = 35.3$ cm, nuclear interaction length $\lambda_{\mathrm{I}} = 42.1$ cm and low density of 1.848 g/cm^3. That results in the energy dissipation along a longer path in the target, decreasing the local heat deposition. In addition, a comparably high melting point of beryllium (1560 K) ensures that the targets do not melt and are operable at high beam intensities.

There is a set of beryllium plates of various lengths, e.g. in CERN North area varying between 4 cm and 50 cm. The need for different lengths results from the fact that the ratio of the electromagnetic shower intensity to the hadronic shower intensity increases linearly with the target length. This is due to the fact that hadron production is a one-step process of the interaction of primary protons with the matter nuclei, as illustrated in Fig. III.14.2. The secondary particles are then exponentially reabsorbed by the target material, hence making the hadron production rate proportional to $L \times e^{-L}$. For the electromagnetic shower, the process has two steps: protons interact with nuclei and produce neutral pions, which in turn decay into two high-energy photons. Those photons can only produce an electromagnetic cascade when they are propagating through the matter. Their reabsorption in target material is exponential, as for the hadrons, hence making the electromagnetic cascade intensity proportional to $L^2 \times e^{-L}$. Plotting both proportionality factors and normalising them to the intensity peak illustrates how the ratio of the electromagnetic cascade intensity to hadronic cascade intensity increases linearly over the material propagation

distance L (see Fig. III.14.3).

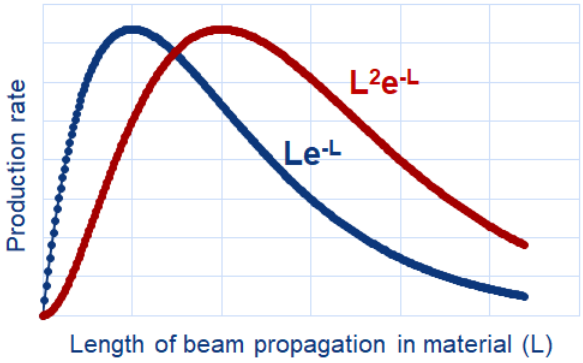

Fig. III.14.3: Normalised curves for hadron production (in blue) and electron production (in red) as a function of beam propagation in the target material [18].

The absolute rates of particle production are notoriously difficult to calculate from fundamentals of Quantum Chromodynamics. Hence, for CERN North Area a phenomenological parametrization has been established by Atherton *et al.* [19] in the framework of data collection of NA20 experiment in 1980. Its result is depicted in Fig. III.14.4. It shows the flux of the secondary particles produced by the primary protons on beryllium target with momentum of 400 GeV/c. The curve represents the flux per solid angle (in steradian), per interacting proton, and per momentum spread (in GeV/c). The diagram depicts the particle production at the zero production angle that is defined as the angle between the direction of the primary proton beam and the secondary beam that is captured by the subsequent beam line. Positive momentum in that diagram represents the production of the positively-charged particles and negative momentum of the negatively-charged particles. The positively-charged particles have a higher flux, especially at higher momenta, due to the positively-charged primary beam.

III.14.3 Secondary beam lines

Experiments and test beams often require “clean” beams of high purity in one particle type and a small momentum spread. The purpose of the secondary beam lines is to collect produced particles from target, select particle momentum and particle type, transport the beam to the experiment and set transverse beam parameters for the experiment. Their design is thoroughly described in Ref. [20] and will be presented here in less detail.

III.14.3.1 Target location

High-energy muons that are generated at low production angles. Muons lose only about 0.5 GeV when propagating through a metre of concrete and about 2 GeV when propagating through a metre of iron, hence for the muons with the energy of 100s of GeV locating the target on ground surface the shielding thickness would need to be in 100s of metres, it would be impractical. Consequently, the CERN North Area targets is located around 10 metres below ground. The typical length of the secondary beam lines at CERN North area is in the order of 1 km. That is in order to permit some of the charged pions, which have a mean decay distance if 56.4 m/(GeV/s) to decay into muons, hence allowing the user the

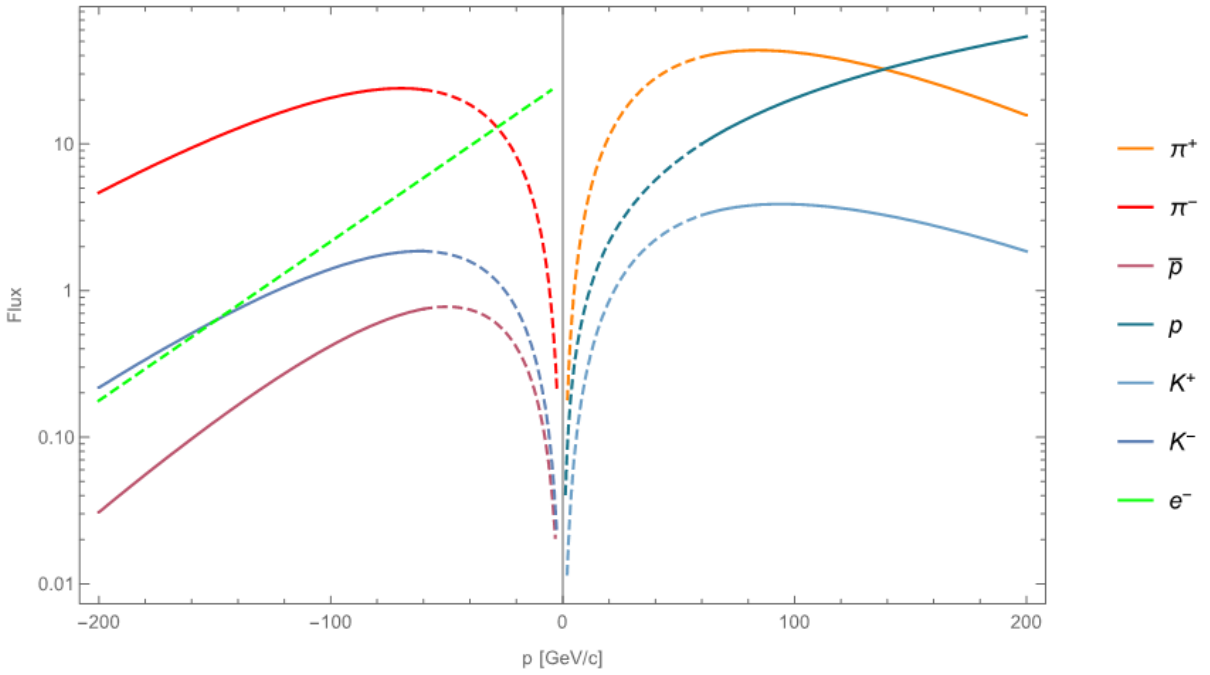

Fig. III.14.4: Production rates as calculated using the 'Atherton' parametrization of NA20 data, expressed per interacting proton, per steradian and per GeV/c [18].

flexibility of selecting the particle type between the pions (that have not yet decayed) and the muons (produced from pions that have already decayed) at the experiment location.

III.14.3.2 Collimation

Directly after the target the beam is collimated with help of a large collimator named TAX (Target Attenuator eXperimental) that limits the transverse emittance of the beam to the acceptance of the beam line that is following it. This way a large share of losses is contained in the well shielded underground region close to the target. The momentum selection is performed by deflecting the beam vertically and generating dispersion. At the location of maximal dispersion there is a vertical focus of the monochromatic beam of selected energy. This way the correlation between the particle momentum and its vertical offset at this location is maximized. A vertical collimator is then used to absorb the particles of deviating energy, and the width of its opening permits to set the momentum spread in the beam line, that can be as low as a fraction of a per mille. After momentum selection, the transverse size and divergence of the beam are set to those required by the experiment via the beam optics settings as well as via collimating the beam with transverse acceptance collimators. Often a one metre long collimator does not suffice to stop the hadron beam, and hence a cleaning collimator is installed downstream of it, in order to remove the tertiary particles produced at the acceptance collimator (see Fig. III.14.5).

As mentioned above, highly energetic muons are difficult to collimate even with many metres of collimator material. For that purpose the muon scrapers and sweepers are utilized (see Fig. III.14.6). These collimators are composed of the magnetic iron, which is magnetized with help of the electric coil. Due to the magnetic field the muons are not only slowed down and scattered, but also deflected out of

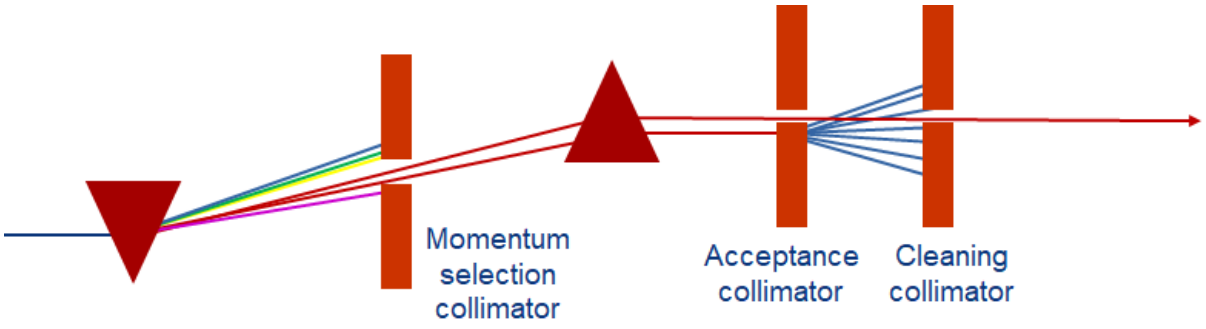

Fig. III.14.5: Illustration of the collimation by momentum selection collimator, acceptance collimator and cleaning collimator. The red triangles indicate the dipole bends.

the beam trajectory and subsequently dumped in the tunnel walls. Scrapers are capable of deflecting the muon beams of a specific polarity, while sweepers collimate muons of both polarities.

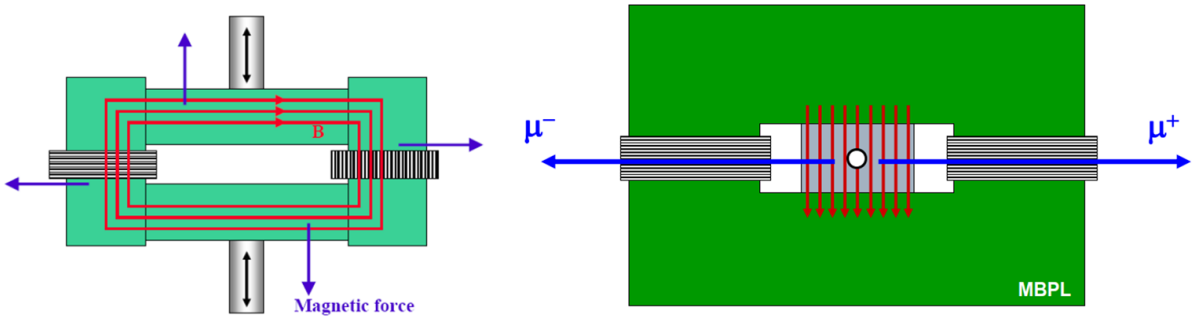

Fig. III.14.6: Illustration of layout and the functionality principle of muon scrapers (left) and sweepers (right) [18].

After the particle production at the target and the subsequent collimation only a small fraction of particle intensity remains. While the primary proton beams from SPS have a momentum of 400 GeV/c and intensities in order of 10^{12}–10^{13} protons per spill, the secondary beam has momenta of hundreds of GeV/c and intensities of up to 10^8 particles per spill. A secondary target producing tertiary beam is also often used, which modifies the particle content and reduces the beam momentum to tens of GeV/c and the intensity to about 10^4 particles per spill.

III.14.3.3 Selecting particle type

A special advantage of the secondary beam lines is the possibility to modify the beam particle type on a comparably short timescale (within seconds or minutes). After the beam interacts with the primary target, a large variety of particles is produced. With the methods described in the present sub-chapter a specific type of particles can be selected to propagate to the experiment.

For production of high-purity electron beam at comparably low energies (tens of GeV), a converter can be used (see Fig. III.14.7). The converter is a thin (order of mm) plate of heavy material (e.g. lead or tungsten). It is moved into the path of the neutral beam after all charged particles have been swept away

by a dipole magnet and have been collimated. The neutral beam consists of neutral hadrons, photons and neutrinos (undetectable with North Area detectors). Photons produce electron-positron pairs in the converter, and subsequently a second dipole is used to bend those electrons or positrons into the direction of the beam line. All other particles are collimated away, hence generating an electron beam of over 99% purity.

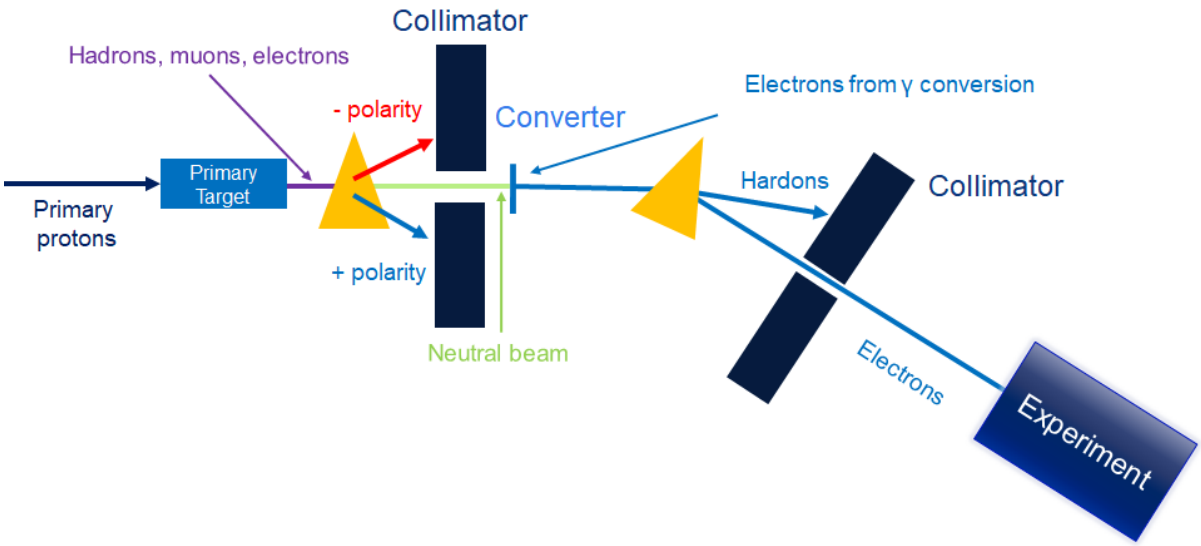

Fig. III.14.7: Illustration of the functionality principle of a converter for low-energy electron production.

Another method is used for generation of high-energy electron beams. Electrons above the energies of 120–150 GeV emit a notable amount of synchrotron radiation when propagating through the dipole bends (per mille to per cent of their energy), while heavier particles in the secondary beam emit much less radiation. The beam line downstream of the dipole can be set to the new reduced electron energy, and the remaining particles are absorbed at the momentum-selection collimator described above. This way only a high-purity high-energy electron beam is transported to the experiment.

In some beam lines it is useful to remove the electrons from the particle mix. For that an absorber (e.g. 6 or 12 mm lead plate) is moved into the beam path (see Fig. III.14.8). This plate causes the electrons and positrons to lose a notable share of their energy via Bremsstrahlung, while the plates are almost transparent for the heavier particles. The electrons are subsequently removed via the tertiary beam momentum selection, that is based on the same principle as that of secondary beams described above.

A so-called radiator can be used to generate a tagged photon beam (see Fig. III.14.9). First, a high-purity electron beam is generated with help of a converter or purified with the synchrotron radiation method described above. Then a radiator—a thin plate of heavy material, similar to that of the converter—is put in the path of this electron beam. Bremsstrahlung photons are created in the radiator and propagate forward towards the experiment. The electrons, on the other hand, are deflected with a dipole magnet and directed towards a monitor that measures the position of their arrival. The timing of arrival of both the photons at the experiment and the electrons at the profile monitor is also measured. It is then used to attribute which photon was generated by which specific electron. The profile monitor acts as a spectrometer, the transverse position of electron arrival gives information on the electron mo-

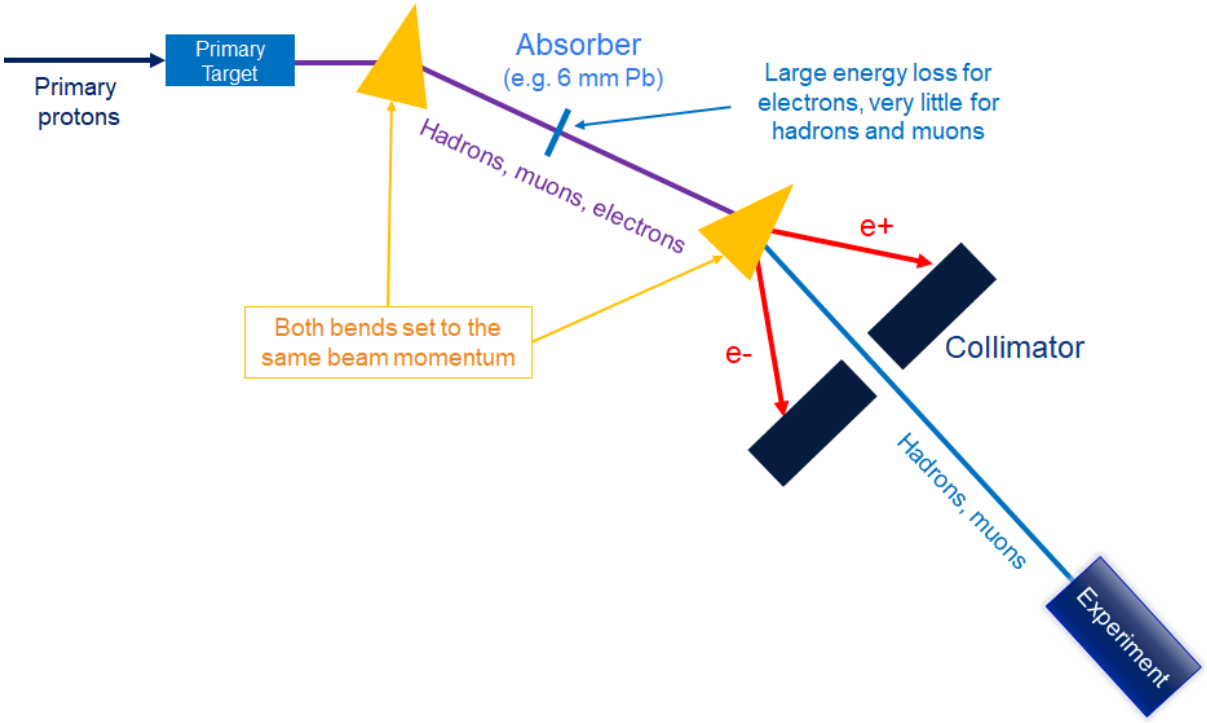

Fig. III.14.8: Illustration of the functionality principle of an absorber used for removal of electrons from the secondary beam.

mentum. The momentum of the photons p_γ can be then calculated as difference between the momentum of the secondary electrons upstream of the radiator p_e and the momentum of the electrons arriving at the profile monitor $p_{e'}$

$$p_\gamma = p_e - p_{e'} \quad . \tag{III.14.1}$$

The result is the tagged photon beam, and in case the experiment aims at examining the interaction of photons with a specific momentum, the analysis can be conducted, selecting only the data corresponding to the photon momentum band of interest.

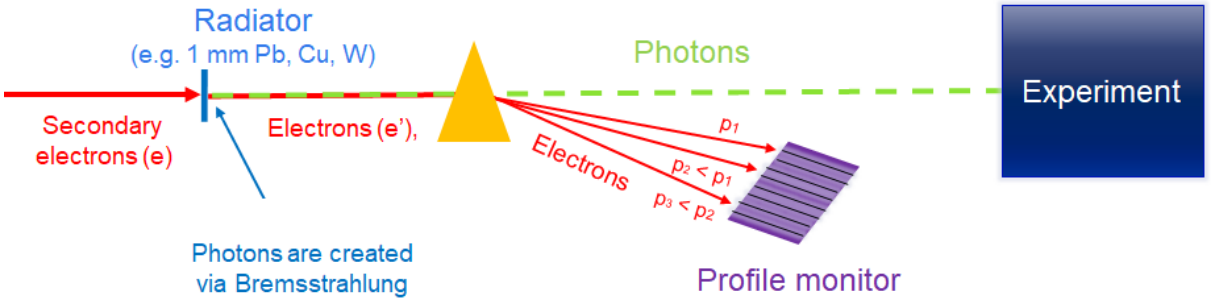

Fig. III.14.9: Illustration of the functionality principle of a radiator used for production of a tagged photon beam.

The final example of beam type purification is the generation of the polarized muon beam that is used by the North Area experiments COMPASS and AMBER (see Fig. III.14.10). This beam generation

is a process composed of several steps that will be only illustrated in general terms here and is described in detail in Ref. [20]. First, the mixed secondary beam of hadrons and leptons is directed from the primary target into a long decay section. The main production channel for muons are the decaying pions and their mean decay distance in CERN North Area is several kilometres, the section has been made comparably long—800 m. In this section all secondary particles—pions, kaons as well as muons that are produced via their decay—are transported along the FODO cells that have been optimized for the maximal momentum acceptance.

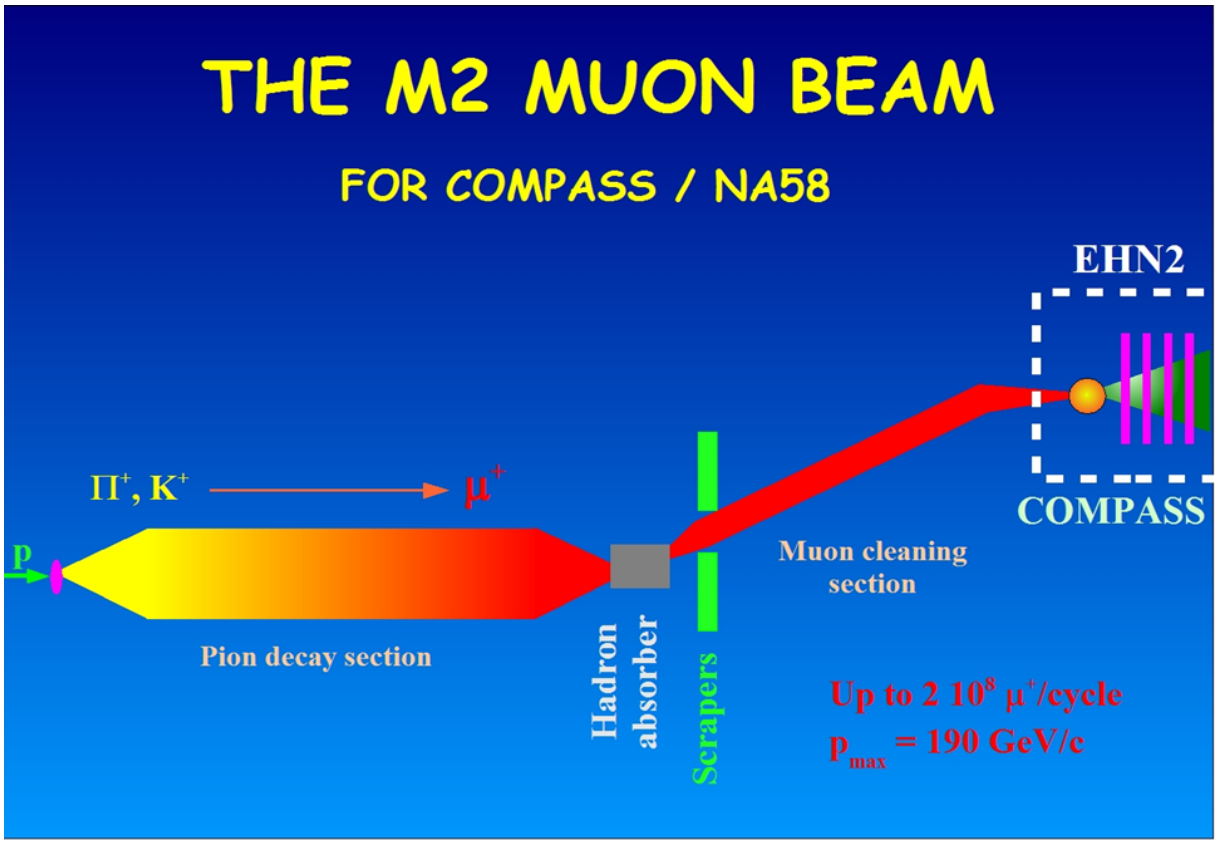

Fig. III.14.10: Schematic of the polarized muons beam line for COMPASS experiment [18].

The main muon production process is a two-body decay of the pions, as illustrated in Fig. III.14.11. The momentum of the muons is between 57% and 100% of the initial momentum of the decaying pions, dependent on the direction of their decay: If in their centre-of-mass frame of reference they decay into the same direction as the initial direction of pion propagation, in the laboratory frame of reference their momentum is almost equal to pion momentum. If the direction of of the muon propagation in centre-of-mass frame of reference is opposite to the initial pion propagation direction, then—in the laboratory frame of reference—the muon has only 57% of the initial pion momentum. Furthermore, the pion is a spin-zero particle. Neutrinos are always left-handed, and so because of the spin conservation the muons that are produced in pion decay are also always left-handed. That implies that their spin is in the opposite direction of their propagation in the center-of-mass frame of reference of the pion decay. Having established that the muon momentum depends on the direction in which it was emitted in pion decay, we can conclude that the muons that are propagating at 100% of pion momentum will have a

negative polarization.

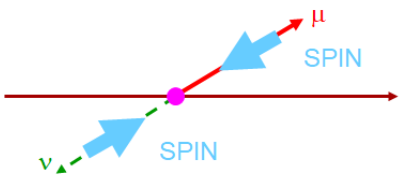

Fig. III.14.11: Diagram illustrating the pion decay into a muon and a neutrino.

III.14.4 Summary

The present chapter has demonstrated a vast number of particle physics experiments that can be performed (only) with fixed targets. Fixed-target particle physics is complementary to collider physics, as the former addresses the intensity frontier and the latter the high-energy frontier of the particle physics exploratory domain. CERN has a rich fixed-target complex that derives its beams from the PSB, PS and SPS accelerators. Those beams range in their momenta from the order of 1 GeV/c to hundreds of GeV/c. The complex is capable of providing a variety of particle types that include protons, electrons, mixed hadrons, pions, tagged kaons, muons, tagged photons and other particle types. The beam lines are designed for high flexibility in particle type, beam size, divergence, momentum, intensity and beam polarization.

Acknowledgements

The author would like to acknowledge Niels Doble, Lau Gatignon as well as the physics team of CERN Experimental Area group (Markus Brugger, Johannes Bernhard, Nikolaos Charitonidis, Dipanwita Banerjee, Maarten van Dijk, Laurie Nevay and others).

References

[1] J.J. Aubert *et al.*, Experimental observation of a heavy particle J, *Phys. Rev. Lett.* **33** (1974) 1404–1406, doi:10.1103/PhysRevLett.33.1404.

[2] J.E. Augustin *et al.*, Discovery of a narrow resonance in e^+e^- annihilation, *Phys. Rev. Lett.* **33** (1974) 1406–1408, doi:10.1103/PhysRevLett.33.1406.

[3] Ch. Fabjan and K. Hübner, in *Technology meets research*, Eds. Ch. Fabjan *et al.* (World Scientific, Singapore, 2017), pp. 87–133 (2017) https://doi.org/10.1142/9789814749145_0004.

[4] R.R. Wilson, The Tevatron, *Phys. Today* **30** (1977) (10) 23–30, doi:10.1063/1.3037746, preprint available as FERMILAB-TM-0763.

[5] J. Beacham *et al.*, Physics Beyond Colliders at CERN: Beyond the Standard Model Working Group report, *J. Phys. G* **47** (2020) 010501, doi:10.1088/1361-6471/ab4cd2.

[6] L. Gatignon, The report of the Conventional Beams Working Group to the Physics Beyond Collider Study and to the European Strategy for Particle Physics, Executive Summary, CERN-PBC-Notes-2018-005 (CERN, Geneva, 2018), doi:10.17181/CERN.8L1V.GFJ6.

[7] R. Alemany *et al.*, Summary report of Physics Beyond Colliders at CERN, CERN-PBC-REPORT-2018-003, arXiv:1902.00260 [hep-ex] (CERN, Geneva, 2018), doi:10.48550/arXiv.1902.00260.

[8] Physics Beyond Colliders Study Group, CERN website, last accessed 28 Feb. 2024, http://cern.ch/pbc.

[9] P. Abbon *et al.*, The COMPASS experiment at CERN, *Nucl. Instrum. Meth. A* **577** (2007) 455–518, doi:10.1016/j.nima.2007.03.026.

[10] B. Adams *et al.*, Letter of intent: A new QCD facility at the M2 beam line of the CERN SPS (COMPASS++/AMBER), CERN-SPSC-2019-003, SPSC-I-250 (CERN, Geneva, 2019), doi:10.48550/arXiv.1808.00848.

[11] N. Antoniou *et al.*, Study of hadron production in hadron–nucleus and nucleus–nucleus collisions at the CERN SPS, CERN-SPSC-2006-034, SPSC-P-330 (CERN, Geneva, 2006), doi:10.17181/CERN.JTNE.Y0QH.

[12] A. Ceccucci *et al.*, Proposal to measure the rare decay $K^+ \to \pi + \nu\overline{\nu}$ at the CERN SPS. CERN-SPSC-2005-013, SPSC-P-326 (CERN, Geneva, 2005), doi:10.17181/CERN.HVBQ.34HD.

[13] Gninenko, S. Proposal for an experiment to search for dark sector particles weakly coupled to muon at the SPS. CERN-SPSC-2019-002, SPSC-P-359 (CERN, Geneva, 2019), doi:10.17181/CERN.LEK5.O4J3.

[14] CLOUD Collaboration, CLOUD : an atmospheric research facility at CERN. physics/0104076 ; CERN-SPSC-2000-041 ; CERN-SPSC-P-317-ADD-2 (CERN, Geneva, 2000), doi:10.17181/CERN.EJX9.HCT3.

[15] Wikimedia Commons, File:Atmospheric Collision.svg, Wikimedia Commons, the free media repository, 2023, accessed 19.02.2024, Wikimedia.

[16] J. Bernhard *et al.*, CERN Proton Synchrotron East Area Facility: Upgrades and renovation during Long Shutdown 2, CERN-2021-004 (CERN, Geneva, 2021), doi:10.23731/CYRM-2021-004.

[17] E. Montbarbon *et al.*, The new CERN East Area primary and secondary beams, Proc. 10th Int. Particle Accelerator Conf. (IPAC2019), Melbourne, Australia, 19–24 May, 2019, THPGW062, doi:10.18429/JACoW-IPAC2019-THPGW062.

[18] D. Banerjee *et al.*, The North Experimental Area at the CERN Super Proton Synchrotron, CERN-ACC-NOTE-2021-0015 (CERN, Geneva, 2021), doi:10.17181/CERN.GP3K.0S1Y.

[19] H.W. Atherton *et al.*, Precise measurements of particle production by 400 GeV/c protons on beryllium targets, CERN-80-07 (CERN, Geneva, 1980), doi:10.5170/CERN-1980-007.

[20] L.Gatignon. Design and tuning of secondary beamlines in the CERN North and East Areas, CERN-ACC-NOTE-2020-0043 (CERN, Geneva, 2020), doi:10.17181/CERN.T6FT.6UDG.